

GigaWorld-Policy: An Efficient Action-Centered World-Action Model

GigaAI

Project Page: <https://gigaai-research.github.io/GigaWorld-Policy/>

GigaWorld Team (alphabetical order): Angen Ye, Boyuan Wang, Chaojun Ni, Guan Huang, Guosheng Zhao, Hao Li, Hengtao Li, Jie Li, Jindi Lv, Jingyu Liu, Min Cao, Peng Li, Qiuping Deng, Wenjun Mei, Xiaofeng Wang, Xinze Chen, Xinyu Zhou, Yang Wang, Yifan Chang, Yifan Li, Yukun Zhou, Yun Ye, Zhichao Liu, Zheng Zhu.

1. INTRODUCTION

Vision-Language-Action (VLA) models (Black et al., 2024; Cen et al., 2025; Cheang et al., 2025; Intelligence et al., 2025; Jiang et al., 2025; Ni et al., 2025; Team et al., 2025; Ye et al., 2025; Zhang et al., 2025) based on Vision-Language Models (VLMs) (Beyer et al., 2024; Marafioti et al., 2025; Steiner et al., 2024) have achieved strong performance. However, a major challenge remains: supervision sparsity. While observations and task conditioning are high-dimensional and semantically rich, action supervision is sparse and low-diversity. As a result, models may rely on contextual shortcuts, collapsing many situations into a small set of action prototypes instead of learning a physically consistent action distribution.

Therefore, some works (Cen et al., 2025; Chang et al., 2025; Ni et al., 2025; Zhang et al., 2025) attempt to inject future-state supervision into existing VLA frameworks by predicting future visual observations, as illustrated in Fig. 2 (a). However, VLM-based VLA (Chen et al., 2025; Cui et al., 2025; Ding et al., 2024, 2025; Li et al., 2025; Team et al., 2026; Tian et al., 2025; Wang et al., 2025; Wu et al., 2025) models are typically optimized for discriminative reasoning rather than high-fidelity generation, making it non-trivial for these additional losses to enforce continuity and physical consistency in the predicted actions.

In contrast, recent efforts incorporate the World Model (WM) from video generation (Liu et al., 2026; Podell et al., 2023; Wang et al., 2025; Ye et al., 2026) into robot policy learning (Bi et al., 2025; Kim et al., 2026; Shen et al., 2025) to further increase supervision density and improve scalability. Leveraging video generation is appealing because it provides temporally dense supervision in the observation space beyond sparse action labels and injects strong spatiotemporal priors learned from large-scale video data. These methods commonly optimize joint objectives of future visual dynamics and action prediction, explicitly coupling future observation forecasting with action selection, thereby leveraging the representational and generative capacity of video models to guide action learning (Fig. 2 (b-c)). However, these approaches often require iterative sampling to roll out future videos at inference time, leading to high latency. Moreover, errors in video prediction can propagate to action decoding, causing mistakes and degraded long-horizon control, particularly when small early inaccuracies compound over time. To address these limitations, we introduce GigaWorld-Policy, an action-centered and efficient World-Action model. Instead of making action prediction overly reliant on explicit video generation, GigaWorld-Policy leverages future visual dynamics as a reasoning signal and a source of dense supervision. Specifically, GigaWorld-Policy is implemented as a causal sequence model that represents action tokens and future-visual tokens under a causal mask. During training, the model learns to predict future

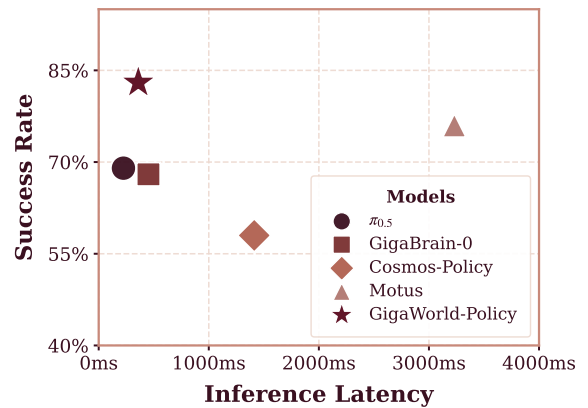


Figure 1: Comparison of GigaWorld-Policy with baselines on inference frequency and task success rate in real-world settings and on an A100 GPU.

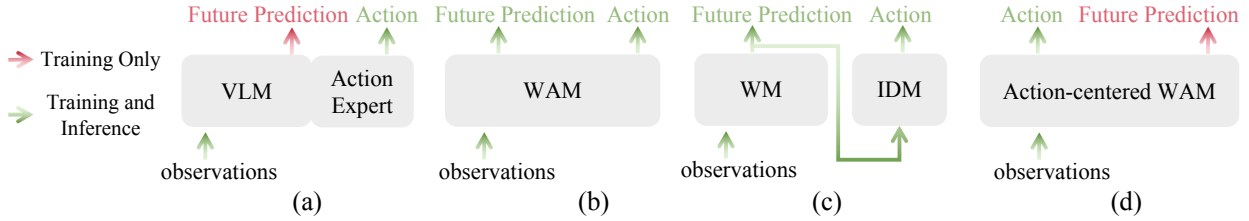


Figure 2: (a) VLM-based VLA with auxiliary future supervision to densify training signals, but limited by the discriminative nature of VLMs (Cen et al., 2025; Ni et al., 2025; Zhang et al., 2025). (b) Joint action–video prediction with bidirectional attention (Bi et al., 2025; Kim et al., 2026; Shen et al., 2025), requiring future video generation at inference. (c) Two-stage design (Pai et al., 2025) that first generates future video and then gets actions via an Inverse Dynamics Model (IDM), inheriting video prediction errors and incurring additional inference cost. (d) GigaWorld-Policy: an action-centered WAM that leverages future visual dynamics as supervision during training, while making future-video prediction optional at inference for low-latency action generation.

action sequences from the current observation context, and in parallel learns an action-conditioned visual dynamics model that forecasts future visual observations given the same current observation together with the predicted actions, thereby coupling action learning with explicit 2D pixel-level state evolution. These two learning signals are optimized within the same model, allowing future visual dynamics to regularize action plausibility and provide substantially denser supervision, which improves learning efficiency. Crucially, at inference time, explicit future-video prediction is optional: the model can be executed in an action-only mode that directly produces control commands without rolling out long sequences of video tokens. This design substantially reduces compute and memory overhead, avoids compounding errors from extended visual rollouts, and enables low-latency closed-loop control, as illustrated in Fig. 2 (d). To obtain stronger pre-trained weights, we use a curriculum training pipeline that injects physics priors from diverse video sources before any task-specific supervision. GigaWorld-Policy is initialized from a large-scale web-video foundation model (Wan et al., 2025), and then further pre-trained on embodied, robot-centric data that combines real robot recordings with large-scale egocentric human videos, improving robustness to embodiment-specific viewpoints and interaction dynamics. Finally, we post-train the model on target-robot trajectories that align images, language, and actions, specializing it for instruction-conditioned action prediction under the target robot’s control interface and state distribution.

We validate GigaWorld-Policy through experiments in both simulation and real-world environments. GigaWorld-Policy outperforms strong baselines, delivering efficiency gains without sacrificing control performance. As shown in Fig. 1, it achieves a trade-off between success and efficiency, delivering $9\times$ faster inference and 7% higher task success rates than the state-of-the-art WAM Motus (Bi et al., 2025). Moreover, under comparable speed and VLA settings, GigaWorld-Policy improves performance by 20%.

The main contributions of this paper are summarized as follows:

- We propose GigaWorld-Policy, an action-centered and efficient World–Action model. During training, future visual dynamics provide dense supervision and a reasoning signal for action learning, without over-reliance on explicit video synthesis. At inference time, future-visual prediction is optional and we can decode actions only, enabling low-latency control.
- We propose a pre-training paradigm that converts a generic video generation model into a strong initialization for robot policy learning, fully leveraging complementary data sources across stages.
- Experiments on real robotic platforms show that GigaWorld-Policy achieves a $9\times$ inference speedup (down to 0.36 s per inference) while improving task success rates by 7% over baseline methods; compared with $\pi_{0.5}$, GigaWorld-Policy matches the inference speed and improves performance by 95% on RoboTwin 2.0.

2. Related Work

2.1. World Models for Robotic Video Generation

Recent advances in world models (Li et al., 2025; Ni et al., 2025; Wang et al., 2025; Zhao et al., 2025) have improved robotic video generation and prediction (Chen et al., 2025; Dong et al., 2025; Liu et al., 2025; Ni et al., 2025; Wang et al., 2025; Zhou et al., 2024). The central goal is to learn a generative model that captures the temporal evolution of the environment, enabling the prediction of future visual sequences.

Pandora (Xiang et al., 2024) proposes a hybrid autoregressive–diffusion world model that generates videos while enabling real-time control via free-text actions. FreeAction (Kim et al., 2025) explicitly exploits continuous action parameters in diffusion-based robot video generation by using action-scaled classifier-free guidance to better control motion intensity. GigaWorld-0-video (Team et al., 2025) is a high-fidelity world-model data engine that synthesizes temporally coherent, high-quality 2D video sequences with fine-grained control over appearance and scene layout. Some methods (Chen et al., 2025) also explore explicit video world models, which aim to construct structured and manipulable 3D scene representations (Liu et al., 2024, 2025; Ni et al., 2025; Wang et al., 2025). Aether (Team et al., 2025) unifies geometry-aware world modeling by jointly optimizing 4D dynamic reconstruction, action-conditioned video prediction, and goal-conditioned visual planning.

However, most existing efforts improve the fidelity, consistency, and controllability of video world models, while largely overlooking how to adapt generic video generators into action-centered models that directly support policy learning under tight latency constraints. In contrast, we treat the video generator as policy initialization and propose an action-centered training recipe that aligns the backbone with robotic observations and action conditioned dynamics.

2.2. World–Action Models for Robotic Control

World–Action Models (WAM) (Bi et al., 2025; Kim et al., 2026; Shen et al., 2025; Wang et al., 2025), grounded in the video generation paradigm, aim to predict robot actions and future visual dynamics within a unified framework. By modeling action-conditioned future observations, WAMs provide dense temporal supervision and a learned predictive prior that regularizes policy learning.

As shown in Fig. 2 (b), VideoVLA (Shen et al., 2025) directly utilizes video generation models as pre-trained weights to explore the transformation of large-scale video generation models into robotic manipulation models, employing multimodal diffusion Transformers to jointly model video, language, and action modalities, achieving dual prediction of actions and future visual outcomes. Motus (Bi et al., 2025) proposes a unified world model that leverages existing general pre-trained models and rich, shareable motion information, introducing a Mixture-of-Transformer (MoT) architecture to integrate three expert modules and adopting a UniDiffuser-style scheduler to enable flexible switching between different modeling modes. In contrast, as shown in Fig. 2 (c), Mimic-video (Pai et al., 2025) adopts a two-stage pipeline: it first leverages an Internet-scale pre-trained video backbone to predict future visual observations, and then uses a flow-matching inverse-dynamics action decoder to map the resulting video latents into low-level robot actions.

However, these methods all typically require iterative diffusion sampling to generate future videos during inference, which introduces significant latency and limits real-time deployment. Meanwhile, an over-reliance on explicit video prediction can be fragile: pixel-level forecasting is sensitive to stochasticity observability, and small visual prediction errors may compound over long horizons, weakening the usefulness of the learned dynamics for robust action generation.

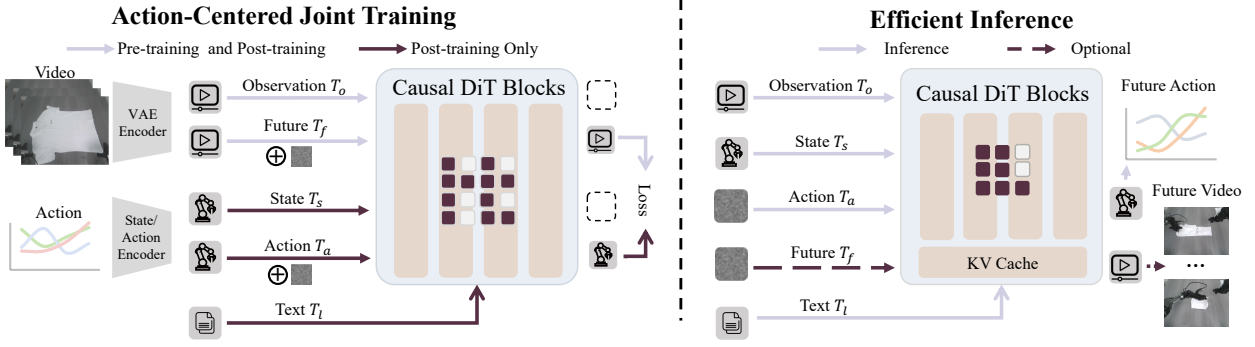


Figure 3: Overview of GigaWorld-Policy, built on a pre-trained video generation backbone. During pre-training, the model learns action-relevant representations from large-scale videos. During post-training for policy learning, it jointly performs action-chunk prediction from the current observation and future video prediction as auxiliary supervision. At inference time, the future-video prediction branch is optional, enabling faster inference.

3. Method

3.1. Problem Statement and Approach Overview

We formulate robotic manipulation as a sequential decision-making task. At each time step t , the robot receives multi-view RGB observations $o_t = \{o_t^v\}_{v \in S}$ from a fixed set of camera viewpoints $S = \{left, front, right\}$, a natural-language instruction l , and the proprioceptive state s_t . Conditioned on these inputs, the policy predicts an action chunk of length p , $a_{t:t+p-1} = (a_t, a_{t+1}, \dots, a_{t+p-1})$.

Vision-Language-Action Policies. Most existing VLA policies are trained via imitation learning to model and sample an action chunk conditioned on the observation, the robot state, and a language instruction:

$$a_{t:t+p-1} \sim q_{\Theta}(\cdot | o_t, s_t, l). \quad (1)$$

The distribution $q_{\Theta}(\cdot | o_t, s_t, l)$ parameterizes the policy over the next p actions. In this paradigm, learning is driven solely by action supervision from demonstrations, without any explicit supervision in the observation space.

Our Approach. Unlike approaches that only model an action distribution, we adopt a world-modeling perspective that learns how visual observations evolve under an executed action chunk. We implement our method as a single unified model g_{Θ} that parameterizes two complementary conditional distributions. For action modeling, anchored by demonstrations, the model learns to sample an action chunk conditioned on the observation, robot state, and language:

$$(a_{t:t+p-1}, c_t) \sim g_{\Theta}(\cdot | o_t, s_t, l), \quad (2)$$

Here, c_t is an action latent conditioning signal that is used to guide visual forecasting. For visual feedforward dynamics modeling, given the same context and the predicted action conditioning signal, the model learns to sample a future observation sequence that captures the evolution of visual observations:

$$(o_{t+\Delta}, o_{t+2\Delta}, \dots, o_{t+K\Delta}) \sim g_{\Theta}(\cdot | o_t, s_t, l, c_t), \quad (3)$$

where Δ denotes the temporal stride between predicted observations, and $K = \lfloor p/\Delta \rfloor$ so that the model predicts $\{o_{t+k\Delta}\}_{k=1}^K$ within the p -step horizon.

3.2. The Architecture of GigaWorld-Policy

As shown in Fig. 3, GigaWorld-Policy adapts a 5B-parameter diffusion Transformer (Wan et al., 2025), pre-trained via an action-centered objective to serve as a World–Action model for robotic manipulation. By concatenating multi-view inputs, the framework enables joint cross-view reasoning with consistency, and uses a causal masking scheme to unify action generation and visual dynamics.

Input Tokens. For visual token inputs, to enable multi-view generation without modifying the backbone while encouraging cross-view consistency, we merge the three camera views into a single composite image of the same resolution as a standard input:

$$o_t^{comp} = Compose(o_t^{left}, o_t^{front}, o_t^{right}). \quad (4)$$

This composite representation preserves the spatial structure of each view in a shared coordinate frame, facilitating cross-view consistency. Meanwhile, since dense frame-by-frame prediction is frequently unnecessary due to strong temporal continuity and redundancy in adjacent observations, we only forecast a sparse set of future frames $\{o_{t+k\Delta}^{comp}\}_{k=1}^K$ using a fixed stride. Concretely, we predict one future observation every Δ steps along the action horizon, which preserves the key evolution of the scene while reducing supervision redundancy.

Shared Transformer Blocks. We then encode both the current observation o_t^{comp} and the predicted future observations $\{o_{t+k\Delta}^{comp}\}_{k=1}^K$ using the same pre-trained Variational Autoencoder (VAE), and tokenize the resulting latents into spatiotemporal visual tokens T_o and T_f . In parallel, we embed proprioceptive states and actions into the pre-trained model’s hidden dimension via linear projections, yielding state tokens T_s and action tokens T_a , respectively. The language instruction l is encoded by a pre-trained language encoder to obtain the instruction token sequence T_l .

Unlike MoE-based designs, we process all token types with a single shared stack of Transformer blocks. In particular, all tokens share the same query, key, and value projection matrices at every layer, which tightly couples action tokens with visual evidence while preserving the computational profile of the pre-trained backbone. Meanwhile, we use different positional encodings for different token types to respect their underlying structures: visual tokens adopt a 2D positional encoding over the image grid, whereas proprioceptive state and action tokens use a 1D temporal positional encoding.

Causal Self-Attention for Video and Action Modeling. To unify action generation and feedforward visual-dynamics modeling within a single diffusion Transformer, we pack all modalities into one token sequence and use a causal attention mask to control information flow. Concretely, at each diffusion step t , we concatenate modality-specific tokens into a unified sequence:

$$T_t = [T_o; T_s; T_a; T_f]. \quad (5)$$

As shown in Fig. 4, we then impose a blockwise causal attention mask to enforce the following dependencies: (i) T_s and T_o may attend to each other, but cannot attend to T_a or T_f ; (ii) action tokens in T_a may attend to the tokens $\{T_s, T_o\}$, but cannot attend to T_f ; (iii) future-video tokens in T_f may attend to $\{T_s, T_o, T_a\}$, enabling feedforward dynamics prediction conditioned on the action chunk. This masking scheme prevents information leakage from predicted future frames into action generation, while allowing future-frame prediction to leverage both observations and actions, consistent with Eq. 2 and Eq. 3.

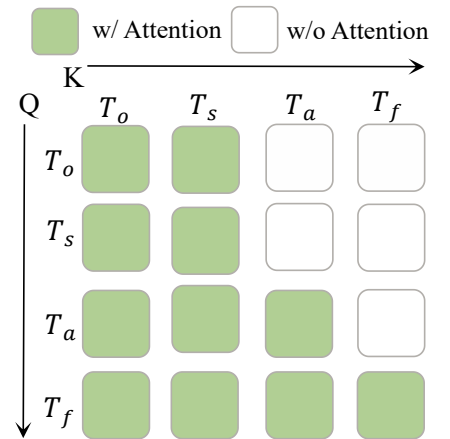


Figure 4: Attention mask for GigaWorld-Policy: action tokens T_a attend to states T_s and current observations T_o only, while future video tokens T_f also attend to actions.

Table 1: Datasets and their estimated collection hours used in embodied data pre-training, covering egocentric human demonstrations and real-world robot manipulation videos.

Dataset	Hours	Dataset	Hours	Dataset	Hours
EgoDex (Hoque et al., 2025)	800	Agibot (Bu et al., 2025)	2,500	EGO4D (Grauman et al., 2022)	3,500
RoboMind (Wu et al., 2024)	300	RDT (Liu et al., 2024)	25	Open X-Embodiment (O’Neill et al., 2024)	3,500
DROID (Khazatsky et al., 2024)	350	ATARA (Feng et al., 2025)	10	Something-Something V2 (Goyal et al., 2017)	200

Notably, the language instruction is not included in the unified self-attention sequence; instead, l is provided as an external conditioning signal via cross-attention, and therefore does not participate in the causal ordering above.

3.3. GigaWorld-Policy: Training

Training Process and Data. We pre-train GigaWorld-Policy to progressively inject physics priors from diverse video sources, enabling the model to acquire generalizable visual-dynamics knowledge before any task-specific supervision.

We first initialize GigaWorld-Policy from a large-scale pretrained video model (Wan et al., 2025), trained on diverse web videos. Building on this foundation, we perform embodied data pre-training, where the model is further pre-trained on robot-centered video data spanning real-world robot videos and large-scale egocentric human videos. On the robot side, we aggregate real-world robot videos from multiple sources (e.g., Agibot (Bu et al., 2025), RDT (Liu et al., 2024), RoboMind (Wu et al., 2024), ATARA (Feng et al., 2025)), which capture robot-specific imaging characteristics, embodiment and workspace constraints, and the distinctive visual patterns induced by arms and end-effectors during interaction. In parallel, we include large-scale egocentric human demonstration videos (e.g., EgoDex (Hoque et al., 2025), Ego4D (Grauman et al., 2022)) to broaden coverage of everyday interaction primitives and long-horizon activity structure, improving robustness to diverse scenes, tools, and task contexts. Overall, as shown in Tab. 1, we collect approximately 10,000 hours of data, and apply unified cleaning, formatting, and sampling across sources to ensure quality and a controllable data distribution. This embodied stage adapts the representation to embodiment-specific viewpoints and manipulation-relevant interaction patterns, improving robustness to viewpoint-induced appearance variations.

After pre-training, the model is post-trained on target-robot task trajectory data that pairs images, language, and actions. This stage specializes the model to the target robot by learning instruction-conditioned action prediction under the robot’s control interface and state distribution.

Training Objective. We use flow matching to optimize both action prediction and visual feedforward dynamics modeling. For either modality x (action tokens or future video tokens), we sample a flow time $s \sim \mathcal{U}(0, 1)$ and noise $\epsilon \sim \mathcal{N}(0, I)$, and construct the interpolated noised variable

$$x^{(s)} = (1 - s)\epsilon + sx, \quad (6)$$

with target velocity:

$$\dot{x}^{(s)} = x - \epsilon. \quad (7)$$

Let z_f denote the VAE latents corresponding to the future observation tokens T_f . We train the model to predict the velocity field of future latents conditioned on history and the executed action chunk:

$$\mathcal{L}_{video} = \mathbb{E}_{s, \epsilon} \left[\left\| g_{\Theta}(z_f^{(s)}, s \mid T_s, T_o, T_a, T_l) - \dot{z}_f^{(s)} \right\|^2 \right]. \quad (8)$$

Similarly, letting a denote the action-token representation for the action chunk T_a , we optimize an action flow-matching objective conditioned on history:

$$\mathcal{L}_{action} = \mathbb{E}_{s, \epsilon} \left[\left\| g_{\Theta}(a^{(s)}, s \mid T_s, T_o, T_l) - \dot{a}^{(s)} \right\|^2 \right]. \quad (9)$$

For pre-training, we optimize only the video flow-matching objective. For post-training, we combine the video and action objectives using scalar weights λ_{video} and λ_{action} to balance their contributions:

$$\mathcal{L}_{all} = \lambda_{video} \mathcal{L}_{video} + \lambda_{action} \mathcal{L}_{action}. \quad (10)$$

3.4. GigaWorld-Policy: Inference

At inference time, our goal is to generate actions with low latency. Directly running the unified video–action diffusion Transformer would require sampling the future video-token stream at every control step, which is costly because video tokens are typically much longer than action tokens. Moreover, predicting future frames is not necessary for executing the policy. We therefore adopt action decoding and optionally decode video, preserving the same backbone and tokenization as in training while avoiding video-generation overhead.

We keep the same conditioning pipeline for language, observations, and proprioception. At each control step t , we first form the context from the instruction, the current proprioceptive state, and the multi-view observation (concatenated as in Eq. 4):

$$w_t = (T_l, T_s, T_o). \quad (11)$$

We then sample only the action chunk tokens T_a from the learned action flow model conditioned on w_t , without instantiating any future video tokens. Concretely, we initialize $a^{(0)} \sim \mathcal{N}(0, I)$ and integrate the learned velocity field from $s = 0$ to $s = 1$:

$$\frac{da^{(s)}}{ds} = g_{\Theta}(a^{(s)}, s \mid w_t), \quad s \in [0, 1], \quad (12)$$

obtaining $a^{(1)}$, which is then decoded to the continuous action chunk $\hat{a}_{t:t+p-1}$. Finally, we execute the action, observe the new state and images, and repeat the above procedure at the next control step. If future prediction is needed, we can enable the video branch at inference time. This can be done either by including the future video tokens in the input and denoising them jointly with the action tokens, or by reusing the KV cache saved during action denoising and then denoising the video tokens conditioned on that cached context.

4. Experiment

Evaluation Metrics. We primarily report the Success Rate (SR) to evaluate task completion performance. In simulation, SR is a binary indicator: $SR = 1$ if the task is completed and $SR = 0$ otherwise. For real-world experiments, we adopt a graded evaluation protocol. Specifically, for the pick-and-place task, we assign a score of 0.5 for a successful grasp and an additional 0.5 for successfully placing the object at the designated target location.

Baselines. We compare GigaWorld-Policy against several state-of-the-art baselines spanning two dominant paradigms. For VLM-based VLA methods, we include $\pi_{0.5}$ (Intelligence et al., 2025), GigaBrain-0 (Team et al., 2025), and X-VLA (Zheng et al., 2025), which leverage large VLM backbones to align visual observations with language instructions and decode low-level control commands via an action head, serving as strong representatives of end-to-end perception-to-action pipelines. For WAM approaches, we evaluate Cosmos-Policy (Kim et al., 2026) and Motus (Bi et al., 2025), which explicitly learn environment dynamics in a latent space and utilize predictive rollouts to support decision making.

Implementation Details. Wan 2.2 5B (Wan et al., 2025) serves as the diffusion-Transformer backbone. We set the action chunk length to $p = 48$, and adopt a future-observation stride of $\Delta = 12$ to provide auxiliary visual-dynamics supervision by sparsely predicting future observations along the action horizon. During post-training, we balance objectives with loss weights $\lambda_{action} = 5$ and $\lambda_{video} = 1$, emphasizing action prediction while retaining the video-consistency regularizer. When reporting inference-time latency, we use the action-only decoding path, where future-video decoding is disabled and the model outputs actions directly. For real-world evaluations, each method is tested with 20 trials per task; in each trial, the robot is allowed up to five attempts

Table 2: Evaluation on RoboTwin 2.0 Simulation. The best results are marked in **bold**, and the second-best results are underlined. GigaWorld-Policy achieves performance comparable to Motus while providing a 9× inference speedup.

Simulation Task	$\pi_{0.5}$		X-VLA		Motus		Our	
	Clean	Rand.	Clean	Rand.	Clean	Rand.	Clean	Rand.
Adjust Bottle	0.79	0.83	1.00	<u>0.99</u>	<u>0.89</u>	0.93	1.00	1.00
Place A2b Left	0.62	0.60	0.48	0.49	<u>0.88</u>	<u>0.79</u>	0.94	0.88
Place Bread Skillet	0.38	0.46	0.77	0.67	<u>0.86</u>	<u>0.83</u>	0.94	0.90
Place Cans Plasticbox	0.40	0.47	0.97	<u>0.98</u>	<u>0.98</u>	0.94	1.00	1.00
Place Fan	0.25	0.36	0.80	0.75	<u>0.91</u>	<u>0.87</u>	0.92	0.94
Place Mouse Pad	0.21	0.26	<u>0.70</u>	<u>0.70</u>	0.66	0.68	0.88	0.90
Place Object Basket	0.43	0.36	0.44	0.39	<u>0.81</u>	<u>0.87</u>	0.90	0.92
Place Object Stand	0.74	0.65	0.86	0.88	<u>0.98</u>	<u>0.97</u>	1.00	0.98
Rotate Qrcode	0.47	0.56	0.34	0.33	<u>0.89</u>	<u>0.73</u>	0.90	0.84
Shake Bottle	0.91	1.00	<u>0.99</u>	1.00	1.00	<u>0.97</u>	1.00	1.00
Stamp Seal	0.36	0.23	0.76	0.82	<u>0.93</u>	<u>0.92</u>	0.96	0.98
Dump Bin Bigbin	0.30	0.42	0.79	0.77	0.95	<u>0.91</u>	<u>0.92</u>	1.00
Handover Block	0.18	0.19	0.73	0.37	0.86	<u>0.73</u>	<u>0.80</u>	0.80
... (50+ tasks in total)								
Handover Mic	0.28	0.18	0.00	0.00	0.78	<u>0.63</u>	<u>0.72</u>	0.72
Move Stapler Pad	0.16	0.18	0.78	0.73	<u>0.83</u>	0.85	0.92	<u>0.82</u>
Open Laptop	0.19	0.35	0.93	1.00	<u>0.95</u>	0.91	0.96	<u>0.98</u>
Place A2b Right	0.62	0.57	0.36	0.36	0.91	<u>0.87</u>	<u>0.90</u>	0.92
Place Burger Fries	0.66	0.70	<u>0.94</u>	0.94	0.98	0.98	0.98	<u>0.96</u>
Place Container Plate	0.71	0.78	<u>0.97</u>	0.95	0.98	0.99	0.98	<u>0.96</u>
Press Stapler	0.80	0.70	0.92	0.98	<u>0.93</u>	0.98	0.96	<u>0.96</u>
Put Object Cabinet	0.24	0.15	0.46	0.48	0.88	<u>0.71</u>	<u>0.74</u>	0.74
Place Dual Shoes	0.12	0.07	0.79	0.88	<u>0.93</u>	<u>0.87</u>	0.96	0.84
Stack Blocks Two	0.48	0.56	<u>0.92</u>	0.87	1.00	0.98	1.00	<u>0.94</u>
Turn Switch	0.05	0.06	0.40	0.61	0.84	<u>0.78</u>	<u>0.82</u>	0.84
Average	0.43	0.44	0.73	0.73	0.89	0.87	<u>0.87</u>	<u>0.85</u>

to finish the task under the same instruction. In simulation, we evaluate each task over 100 test episodes.

4.1. Inference Speed Comparison

To assess deployment efficiency, we benchmark per-step inference latency on an NVIDIA A100 GPU. As summarized in Tab. 3, we report inference time together with success rates in simulation and in the real world. GigaWorld-Policy is substantially faster than prior World–Action models, achieving an approximately 9× speedup over Motus (Bi et al., 2025) while maintaining comparable simulation performance and improving real-world success. Compared with the strong VLA baselines, GigaWorld-Policy trades a modest increase in latency for markedly better simulation success and

a large gain in real-world performance, while remaining close to real-time operation. Overall, these results suggest that GigaWorld-Policy strikes a favorable balance between world-model-based capability and practical

Table 3: Inference latency on an NVIDIA A100, and Success Rate in simulation and real world. The best results are marked in **bold**, and the second-best results are underlined.

Method	Time (ms)	SR in Simulation	SR in Real-World
Vision–Language–Action Models			
$\pi_{0.5}$ (Intelligence et al., 2025)	225	0.48	0.69
GigaBrain-0 (Team et al., 2025)	452	–	0.68
World–Action Models			
Motus (Bi et al., 2025)	3231	0.88	<u>0.76</u>
Cosmos-Policy (Kim et al., 2026)	1413	–	0.58
Ours	<u>360</u>	<u>0.86</u>	0.83

Table 4: Comparison of task success rates in real-world experiments. The best results are marked in **bold**, and the second-best results are underlined.

Method	Clean the Desk	Scan a QR Code	Sweep up Trash	Stack Bowls	Average
Vision–Language–Action Models					
$\pi_{0.5}$ (Intelligence et al., 2025)	0.75	0.55	0.65	<u>0.80</u>	0.69
GigaBrain-0 (Team et al., 2025)	0.70	<u>0.65</u>	0.60	0.75	0.68
World–Action Models					
Motus (Bi et al., 2025)	<u>0.80</u>	0.75	<u>0.70</u>	<u>0.80</u>	<u>0.76</u>
Cosmos-Policy (Kim et al., 2026)	0.65	0.50	0.45	0.70	0.58
Our	0.90	0.75	0.75	0.90	0.83

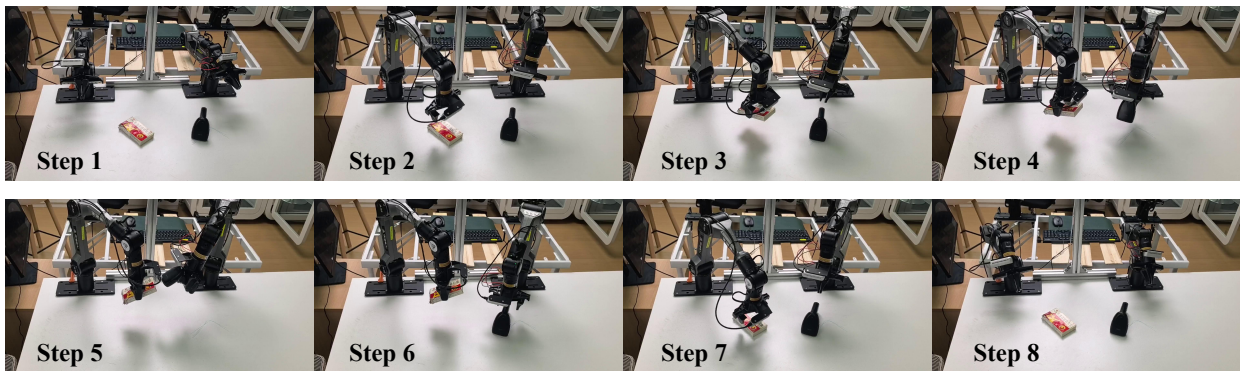


Figure 5: Real-world deployment of GigaWorld-Policy on PiPER arms for QR code scanning.

inference efficiency.

4.2. Simulation Benchmark Experiments

Simulation Setup. We evaluate single-task performance on RoboTwin 2.0 (Chen et al., 2025) over 50 representative manipulation tasks under domain randomization. To assess cross-task generalization and the effect of pre-training, we train all baselines and GigaWorld-Policy on a mixed dataset of 2,500 demonstrations from clean scenes (50 per task) and 25,000 demonstrations from heavily randomized scenes (500 per task). Randomization includes backgrounds, table clutter, table height perturbations, and lighting changes, testing robustness to distribution shifts.

Results. As shown in Tab. 2, GigaWorld-Policy improves the average success rate by over 44 percentage points compared with the $\pi_{0.5}$ (Intelligence et al., 2025) model in the RoboTwin 2.0 (Chen et al., 2025) multi-task setting. Despite achieving an $9\times$ inference speedup, GigaWorld-Policy attains performance comparable to Motus (Bi et al., 2025). These results suggest that our action-centered World–Action modeling paradigm strengthens policy learning via joint supervision, combining action prediction with a visual-dynamics consistency auxiliary constraint during training to better align learned representations with downstream control. At inference time, GigaWorld-Policy makes future-video prediction optional, enabling low-latency action generation and largely accelerating inference without sacrificing overall task performance.

4.3. Real-World Experiment

To evaluate real-world effectiveness, we conducted gripper-based manipulation experiments on an AgileX PiPER 6-DoF robotic arm. We further designed four real-world tasks—Clean the Desk, Scan a QR Code, Stack Bowls, and Sweep up Trash—with detailed descriptions provided in the supplementary material. As summarized in

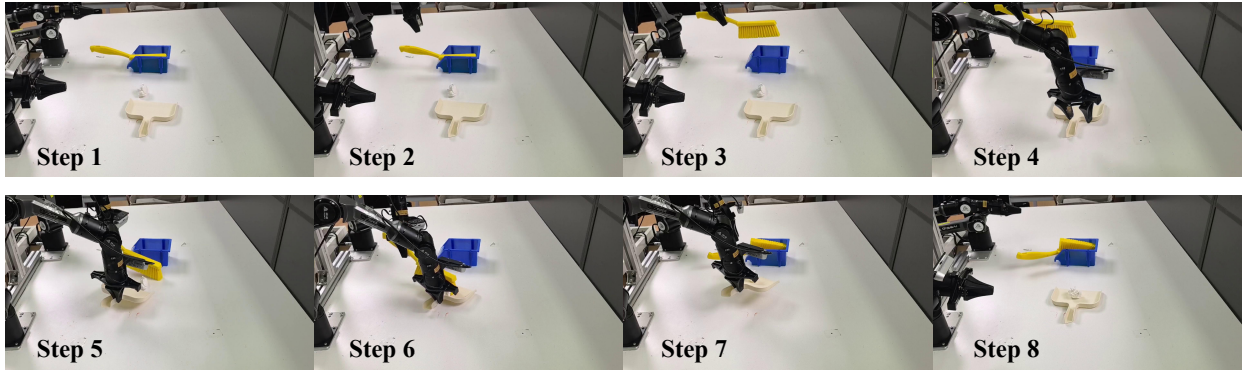


Figure 6: Real-world deployment of GigaWorld-Policy on PiPER arms for trash sweeping.

Table 5: Effect of the sampling interval Δ on real-world task Success Rate. The model predicts $K = \lfloor 48/\Delta \rfloor$ future frames. $K = 0$ indicates no future video prediction. The best results are marked in **bold**, and the second-best results are underlined.

Δ	0	4	8	12	24	48
Success Rate \uparrow	0.60	0.76	<u>0.78</u>	0.83	0.80	0.76

Tab. 4, GigaWorld-Policy achieves stronger overall performance than representative world-model-based robot policies. Notably, although GigaWorld-Policy runs nine times faster than Motus (Bi et al., 2025), it still attains a 7% higher success rate. We attribute this advantage to the tight coupling between success and execution efficiency in real deployments: slower inference introduces control latency, reduces the effective action update rate, and weakens closed-loop error correction. GigaWorld-Policy also maintains a clear advantage over VLA baselines: compared with $\pi_{0.5}$ (Intelligence et al., 2025), it improves the average real-world success rate by about 14% and achieves consistently higher success across all four tasks.

4.4. Data Efficiency

Collecting real-world robot data is expensive, making sample-efficient policy learning critical. We study the data efficiency of GigaWorld-Policy and compare it against a VLA baseline. For each real-world task, we subsample the training demonstrations to multiple fractions, train all methods under the same setting, and evaluate success rates using the same protocol. As shown in Fig. 7, conditioning on the video-prior representations learned by our World–Action model yields an improvement in sample efficiency. Specifically, GigaWorld-Policy reaches the maximum success rate achieved by the VLA using only 10% of the training data.

4.5. Ablation Study

In this section, we conduct real-world ablation studies to isolate the contribution of each component to task success and robustness.

Importance of Pre-training. We analyze our pre-training pipeline by ablating its components. Specifically, we compare four post-training settings: (i) training from scratch without any pre-training, (ii) initializing from the pretrained video model without embodied data pre-training, (iii) using only embodied data pre-training (without video-model initialization), and (iv) initializing from the same pretrained video model after applying embodied data pre-training. As shown in Tab. 7, training from scratch achieves an SR of 0.45. Pretrained video initialization improves SR to 0.57, while using only embodied data pre-training yields 0.73. Combining both delivers the best result, indicating that they provide complementary benefits.

We also study how the amount of data used for embodied-data pre-training affects performance. We keep the pretrained video initialization and all post-training settings fixed, and vary the fraction of data in embodied data

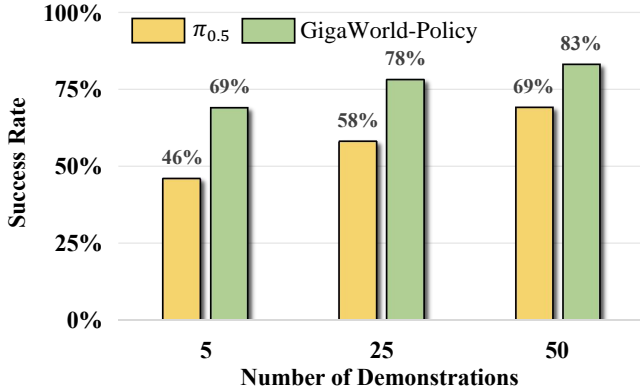


Figure 7: Success rate as a function of training data fraction on real-world tasks. GigaWorld-Policy matches the $\pi_{0.5}$ with only 10% of the data.

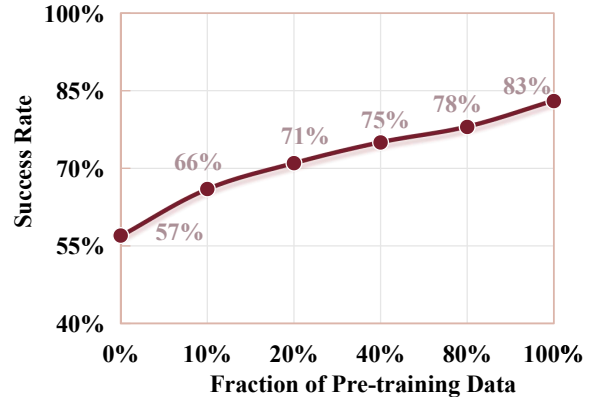


Figure 8: Increasing the fraction of embodied data pre-training consistently improves real-world success.

Table 6: Ablation study on the causal self-attention mask. We report SR and generation quality on the real-world test set. The best results are **bold**.

Method	SR \uparrow	PSNR \uparrow	SSIM \uparrow
Self-Attn	0.81	27.87	0.892
Ours	0.83	28.41	0.901

Table 7: Effect of different pre-training configurations on SR.

Pretrained Init	Embodied Data Pre-training	SR \uparrow
		0.45
\checkmark		0.57
	\checkmark	0.73
\checkmark	\checkmark	0.83

pre-training. As shown in Fig. 8, increasing the embodied data fraction steadily improves real-world success, from 57% without embodied pre-training to 83% with the full dataset. We observe a clear and consistent improvement as the embodied pre-training data scales up, suggesting that increasing embodied coverage further strengthens the learned action-relevant representations and translates into higher real-world success.

Impact of the Number of Predicted Future Frames. We study whether feed-forward dynamics modeling improves action understanding and execution. As shown in Tab. 5, we fix the action chunk length to 48 and vary the number of predicted future frames by adjusting the sampling interval Δ . Under this setting, the model predicts $K = \lfloor 48/\Delta \rfloor$ future frames. When $K = 0$, the model performs no future video prediction and degenerates to an action decoder conditioned only on the current observation. The results demonstrate a consistent improvement in success rate once feed-forward dynamics modeling is enabled, with performance increasing from 0.65 to 0.83, yielding an absolute gain of 0.18. This suggests that anticipating future observations provides useful temporal priors for decision making, leading to more accurate and stable action execution. Meanwhile, we find that predicting denser future videos does not yield additional gains. This suggests that, a moderate amount of future modeling is sufficient to provide useful information for action prediction, while overly long prediction horizons exhibit diminishing returns and may even degrade performance.

Role of Causal Self-Attention for Video–Action Modeling. We ablate the self-attention mask. Our causal design prevents leakage by restricting action tokens to attend only to the state and current observation. We compare this causal mask with a self-attention variant. In the self-attention variant, all tokens can attend to each other without constraints. As shown in Tab. 6, both achieve similar SR under matched settings. However, causal self-attention is more deployable: it ensures the video prediction is optional at inference. We also compare future video generation quality on a held-out real-world test set from the target platform, using standard reconstruction metrics. As shown in Tab. 6, our method achieves higher PSNR and SSIM; furthermore, in Fig. 9, the red boxed regions indicate that our method more accurately predicts fine-grained object state and appearance changes. We attribute this improvement to the proposed causal masking, which

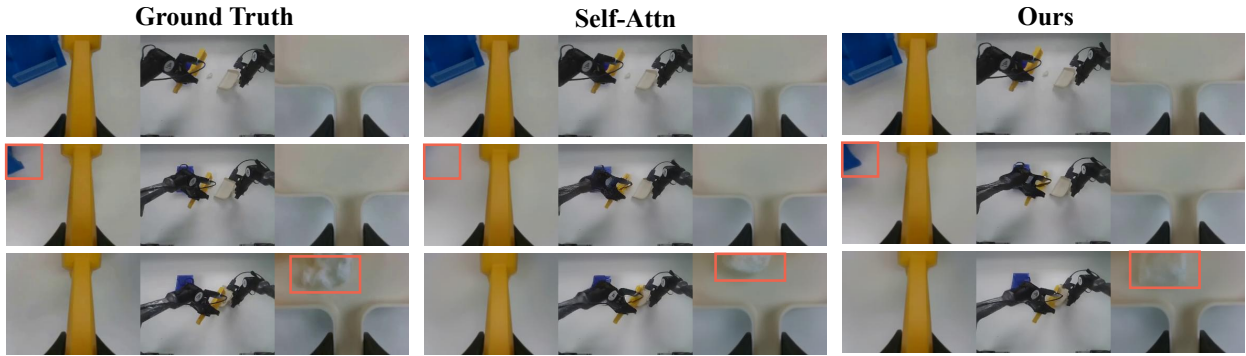


Figure 9: Qualitative comparison between the self-attention baseline and our method. In the red boxes, our method more accurately predicts object state changes.

enforces a physically meaningful factorization between action prediction and forward visual dynamics. Under unconstrained self-attention, action tokens may attend to future-frame tokens during training, introducing information leakage that weakens action-conditioned dynamics learning.

5. Conclusion

We introduced GigaWorld-Policy, an action-centered World–Action Model built on an action-conditioned video generation backbone pre-trained on a curated, multi-level large-scale robot dataset. By decomposing policy learning into future action sequence prediction together with action-conditioned video generation during training, GigaWorld-Policy learns 2D pixel–action dynamics with richer supervision, producing more accurate and plausible action plans. Experiments on real-world robotic platforms show that GigaWorld-Policy reduces inference overhead while improving task performance, achieving a $9\times$ inference speedup (down to 0.36 s per inference) and up to a 7% increase in task success rates over prior baselines.

Supplementary Material for GigaWorld-Policy: An Efficient Action-Centered World–Action Model

A. Implementation Details.

Baselines. We compare SwiftWA with representative baselines from two dominant paradigms: VLM-based VLA methods, including $\pi_{0.5}$ [Intelligence et al. \(2025\)](#), GigaBrain-0 [Team et al. \(2025\)](#), and X-VLA [Zheng et al. \(2025\)](#), and World-Action Models, including Cosmos-Policy [Kim et al. \(2026\)](#) and Motus [Bi et al. \(2025\)](#).

$\pi_{0.5}$ [Intelligence et al. \(2025\)](#) is a vision-language-action (VLA) model built upon π_0 for open-world robotic generalization. It leverages co-training on heterogeneous tasks and diverse supervision sources, including data from multiple robots, high-level semantic prediction, web data, and low-level robot actions, enabling broader transfer to real-world manipulation scenarios. The model is initialized from a web-pretrained vision-language model and trained to combine high-level semantic reasoning with low-level control. Similar to π_0 , the final policy uses Flow Matching to predict continuous action chunks for efficient real-time robot control.

X-VLA [Zheng et al. \(2025\)](#) is a scalable cross-embodiment vision-language-action model that introduces embodiment-specific soft prompts to handle heterogeneity across diverse robotic data sources. Built on a shared Transformer backbone, it uses separate sets of learnable prompt embeddings for different robots or data domains, enabling efficient adaptation with minimal additional parameters while preserving generalization across embodiments. The model is designed for large-scale pretraining on heterogeneous robot datasets, and its final policy employs Flow Matching for continuous action prediction.

GigaBrain-0 [Team et al. \(2025\)](#) is a vision-language-action (VLA) foundation model that leverages world model-generated data to reduce reliance on large-scale real-world robot data. By incorporating diverse generated data, RGBD input modeling, and embodied Chain-of-Thought supervision, it improves cross-task generalization and robustness in dexterous, long-horizon, and mobile manipulation tasks.

Motus [Bi et al. \(2025\)](#) is a unified latent action world model that integrates understanding, video generation, and action modeling within a single Mixture-of-Transformer architecture. By learning latent actions from optical flow and supporting flexible mode switching through a UniDiffuser-style scheduler, it enables large-scale pretraining on heterogeneous data and achieves strong performance in both simulation and real-world robotic tasks.

Cosmos-Policy [Kim et al. \(2026\)](#) is a robot policy that fine-tunes a pretrained video model for visuomotor control and planning in a single post-training stage without architectural changes. It directly generates actions, future state images, and value estimates as latent frames within the model’s latent diffusion process, enabling both policy learning and test-time planning with strong performance in simulation and real-world manipulation tasks.

Pretraining Details. We pretrain our model on public datasets for 6000 GPU hours using a global batch size of 256. We use the AdamW optimizer with $\beta_1 = 0.85$ and $\beta_2 = 0.9$. The learning rate follows a cosine decay schedule, with an initial value of 1×10^{-4} and a final value of 1×10^{-6} .

B. More details about the simulation experiments.

Tab. 8 summarizes the evaluation results on the RoboTwin 2.0 simulation benchmark, where Motus and other baselines are tested on all 50 tasks under both clean and randomized scenes. This setup enables a thorough comparison of their effectiveness in standard conditions and their robustness when facing changes in scene configurations.

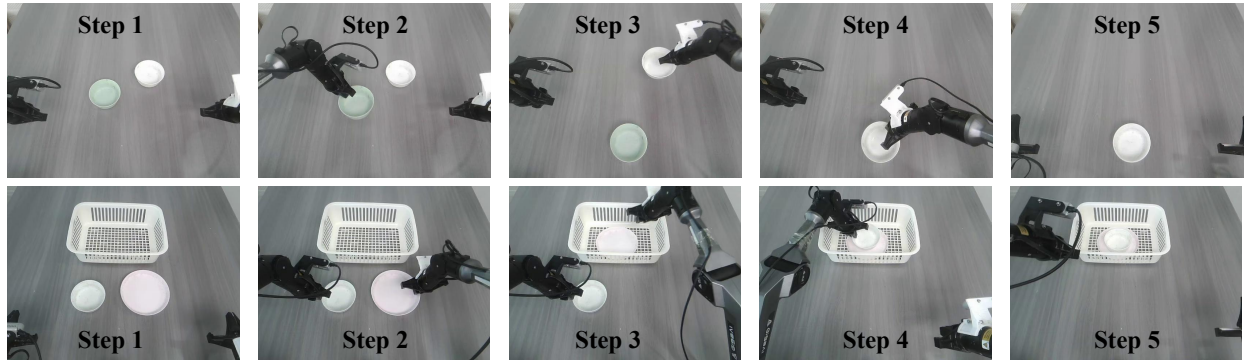


Figure 10: Real-world deployment of GigaWorld-Policy on PiPER arms for stacking bowls and cleaning a desk.

C. More details about the real world experiments.

As shown in Fig. 5, Fig. 6 and Fig. 10, we illustrate the real-world scenarios and tasks used in our experiments, covering four manipulation tasks. For each task, we collect 50 demonstration trajectories, which are then used for post-training. The tasks are described as follows:

Clean the desk: The workspace contains a collection of bowls and plates with stochastically assigned color attributes, interspersed with randomly distributed obstacle objects. The robot is required to sequentially grasp and relocate all tableware items into a target basket, while satisfying a geometric ordering constraint that mandates plates be placed beneath bowls.

Stack bowls: Two bowls are initialized at arbitrary poses on the tabletop surface. The robot must identify and manipulate both objects to produce a properly nested configuration, with one bowl seated securely atop the other.

Scan a QR code: A QR code is affixed to a target object, which is placed at a randomized location within the workspace. The robot must first pick up a handheld scanner, then grasp the target object, align the scanner with the object’s QR code to successfully read it, and finally return the object to its original location. This task evaluates the robot’s capabilities in multi-step task planning, tool use, and precise visual alignment for reliable decoding.

Sweep up Trash: Small objects are randomly scattered on a flat surface. The robot must first pick up a brush-like tool and a dustpan, then sweep the dispersed items into the dustpan using coordinated pushing motions. This task requires sustained contact force control and adaptive trajectory adjustment in response to the disordered initial configuration of the objects.

Table 8: Evaluation on RoboTwin 2.0 Simulation. The best results are marked in **bold**, and the second-best results are underlined. GigaWorld-Policy achieves performance comparable to Motus while providing a 9× inference speedup.

Simulation Task	$\pi_{0.5}$		X-VLA		Motus		Our	
	Clean	Rand.	Clean	Rand.	Clean	Rand.	Clean	Rand.
Adjust Bottle	0.79	0.83	1.00	<u>0.99</u>	<u>0.89</u>	0.93	1.00	1.00
Beat Block Hammer	0.63	0.50	0.92	<u>0.88</u>	0.95	0.88	<u>0.86</u>	<u>0.86</u>
Blocks Ranking Rgb	0.43	0.35	0.83	0.83	0.99	0.97	<u>0.92</u>	<u>0.96</u>
Blocks Ranking Size	0.08	0.14	<u>0.67</u>	0.74	0.75	<u>0.63</u>	0.44	<u>0.48</u>
Click Alarmclock	0.97	0.93	<u>0.99</u>	0.99	1.00	1.00	1.00	1.00
Click Bell	0.75	0.76	1.00	1.00	1.00	1.00	1.00	1.00
Dump Bin Bigbin	0.30	0.42	0.79	0.77	0.95	<u>0.91</u>	<u>0.92</u>	1.00
Grab Roller	0.90	0.89	1.00	1.00	1.00	1.00	1.00	1.00
Handover Block	0.18	0.19	0.73	0.37	0.86	0.73	<u>0.80</u>	0.80
Handover Mic	0.28	0.18	0.00	0.00	0.78	0.63	<u>0.72</u>	<u>0.72</u>
Hanging Mug	0.03	0.03	<u>0.23</u>	<u>0.27</u>	0.38	0.38	0.16	0.12
Lift Pot	0.00	0.00	0.99	1.00	0.96	<u>0.99</u>	<u>0.98</u>	<u>0.98</u>
Move Can Pot	0.29	0.27	0.89	0.86	0.34	<u>0.74</u>	<u>0.76</u>	<u>0.78</u>
Move Pillbottle Pad	0.33	0.29	0.73	0.71	0.93	0.96	<u>0.90</u>	<u>0.90</u>
Move Playingcard Away	0.59	0.67	<u>0.93</u>	0.98	1.00	<u>0.96</u>	0.78	<u>0.72</u>
Move Stapler Pad	0.16	0.18	0.78	0.73	<u>0.83</u>	0.85	0.92	<u>0.82</u>
Open Laptop	0.19	0.35	0.93	1.00	<u>0.95</u>	0.91	0.96	<u>0.98</u>
Open Microwave	0.35	0.37	<u>0.79</u>	<u>0.71</u>	0.95	0.91	0.74	<u>0.66</u>
Pick Diverse Bottles	0.05	0.03	<u>0.58</u>	<u>0.36</u>	0.90	0.91	<u>0.82</u>	0.70
Pick Dual Bottles	0.10	0.06	0.47	0.36	0.96	0.90	<u>0.86</u>	<u>0.86</u>
Place A2b Left	0.62	0.60	0.48	0.49	<u>0.88</u>	<u>0.79</u>	0.94	0.88
Place A2b Right	0.62	0.57	0.36	0.36	<u>0.91</u>	<u>0.87</u>	0.90	0.92
Place Bread Basket	0.48	0.56	0.81	0.71	<u>0.91</u>	0.94	<u>0.82</u>	<u>0.82</u>
Place Bread Skillet	0.38	0.46	0.77	0.67	<u>0.86</u>	<u>0.83</u>	0.94	0.90
Place Burger Fries	0.66	0.70	0.94	0.94	0.98	0.98	0.98	<u>0.96</u>
Place Can Basket	0.19	0.25	0.49	0.52	0.81	0.76	<u>0.78</u>	<u>0.74</u>
Place Cans Plasticbox	0.40	0.47	<u>0.97</u>	<u>0.98</u>	<u>0.98</u>	0.94	1.00	1.00
Place Container Plate	0.71	0.78	<u>0.97</u>	<u>0.95</u>	0.98	<u>0.96</u>	0.98	0.96
Place Dual Shoes	0.12	0.07	0.79	<u>0.88</u>	<u>0.93</u>	0.87	0.96	0.84
Place Empty Cup	0.75	0.86	1.00	0.98	<u>0.99</u>	<u>0.98</u>	0.90	<u>0.90</u>
Place Fan	0.25	0.36	0.80	0.75	<u>0.91</u>	<u>0.87</u>	0.92	0.94
Place Mouse Pad	0.21	0.26	<u>0.70</u>	<u>0.70</u>	<u>0.66</u>	<u>0.68</u>	0.88	0.90
Place Object Basket	0.43	0.36	<u>0.44</u>	<u>0.39</u>	<u>0.81</u>	<u>0.87</u>	0.90	0.92
Place Object Scale	0.40	0.49	0.52	<u>0.74</u>	0.88	<u>0.85</u>	0.88	0.80
Place Object Stand	0.74	0.65	0.86	0.88	<u>0.98</u>	<u>0.97</u>	1.00	0.98
Place Phone Stand	0.49	0.53	0.88	0.87	<u>0.87</u>	<u>0.86</u>	0.82	0.72
Place Shoe	0.57	0.61	0.96	0.95	<u>0.99</u>	<u>0.97</u>	0.98	0.96
Press Stapler	0.80	0.70	0.92	<u>0.98</u>	<u>0.93</u>	0.98	0.96	<u>0.96</u>
Put Bottles Dustbin	0.12	0.09	0.74	0.77	0.81	<u>0.79</u>	0.72	<u>0.70</u>
Put Object Cabinet	0.24	0.15	0.46	0.48	0.88	0.71	0.74	0.74
Rotate Qrcode	0.47	0.56	0.34	0.33	<u>0.89</u>	0.73	0.90	<u>0.84</u>
Scan Object	0.42	0.38	0.14	0.36	0.67	0.66	<u>0.60</u>	<u>0.64</u>
Shake Bottle Horizontally	0.96	1.00	1.00	1.00	1.00	<u>0.98</u>	1.00	<u>0.98</u>
Shake Bottle	0.91	1.00	0.99	1.00	1.00	<u>0.97</u>	1.00	1.00
Stack Blocks Three	0.15	0.16	0.06	0.10	0.91	0.95	<u>0.70</u>	<u>0.78</u>
Stack Blocks Two	0.48	0.56	0.92	0.87	<u>0.99</u>	<u>0.98</u>	1.00	0.94
Stack Bowls Three	0.33	0.35	<u>0.76</u>	0.86	<u>0.79</u>	<u>0.87</u>	0.70	0.72
Stack Bowls Two	0.78	0.66	0.96	0.93	0.98	0.98	<u>0.96</u>	<u>0.92</u>
Stamp Seal	0.36	0.23	0.76	0.82	<u>0.93</u>	<u>0.92</u>	0.96	0.98
Turn Switch	0.05	0.06	0.40	<u>0.61</u>	0.84	<u>0.78</u>	<u>0.82</u>	0.84
Average	0.43	0.44	0.73	0.73	0.89	0.87	<u>0.86</u>	<u>0.85</u>

References

- [1] Lucas Beyer, Andreas Steiner, André Susano Pinto, Alexander Kolesnikov, Xiao Wang, Daniel Salz, Maxim Neumann, Ibrahim Alabdulmohsin, Michael Tschannen, Emanuele Bugliarello, et al. Paligemma: A versatile 3b vlm for transfer. *arXiv preprint arXiv:2407.07726*, 2024. 1
- [2] Hongzhe Bi, Hengkai Tan, Shenghao Xie, Zeyuan Wang, Shuhe Huang, Haitian Liu, Ruowen Zhao, Yao Feng, Chendong Xiang, Yinze Rong, et al. Motus: A unified latent action world model. *arXiv preprint arXiv:2512.13030*, 2025. 1, 2, 3, 7, 8, 9, 10, 13
- [3] Kevin Black, Noah Brown, Danny Driess, Adnan Esmail, Michael Equi, Chelsea Finn, Niccolo Fusai, Lachy Groom, Karol Hausman, Brian Ichter, et al. pi0: A vision-language-action flow model for general robot control. *arXiv preprint arXiv:2410.24164*, 2024. 1
- [4] Qingwen Bu, Jisong Cai, Li Chen, Xiuqi Cui, Yan Ding, Siyuan Feng, Xindong He, Xu Huang, et al. Agibot world colosseum: A large-scale manipulation platform for scalable and intelligent embodied systems. In *IROS*, 2025. 6
- [5] Jun Cen, Chaohui Yu, Hangjie Yuan, Yuming Jiang, Siteng Huang, Jiayan Guo, Xin Li, Yibing Song, Hao Luo, Fan Wang, et al. Worldvla: Towards autoregressive action world model. *arXiv preprint arXiv:2506.21539*, 2025. 1, 2
- [6] Yifan Chang, Jie Qin, Limeng Qiao, Xiaofeng Wang, Zheng Zhu, Lin Ma, and Xingang Wang. Scalable training for vector-quantized networks with 100% codebook utilization. *arXiv preprint arXiv:2509.10140*, 2025. 1
- [7] Chilam Cheang, Sijin Chen, Zhongren Cui, Yingdong Hu, Liqun Huang, Tao Kong, Hang Li, Yifeng Li, Yuxiao Liu, Xiao Ma, et al. Gr-3 technical report. *arXiv preprint arXiv:2507.15493*, 2025. 1
- [8] Kaixiang Chen, Pengfei Fang, and Hui Xue. Depro: Domain ensemble using decoupled prompts for universal cross-domain retrieval. In *Proceedings of the 48th International ACM SIGIR Conference on Research and Development in Information Retrieval, SIGIR '25*, page 958–967, 2025. 1
- [9] Kaixiang Chen, Pengfei Fang, and Hui Xue. Multi-modal interactive agent layer for few-shot universal cross-domain retrieval and beyond. In *The Thirty-ninth Annual Conference on Neural Information Processing Systems*, 2025. 1
- [10] Tianxing Chen, Zanxin Chen, Baijun Chen, Zijian Cai, Yibin Liu, Qiwei Liang, Zixuan Li, Xianliang Lin, Yiheng Ge, Zhenyu Gu, et al. Robotwin 2.0: A scalable data generator and benchmark with strong domain randomization for robust bimanual robotic manipulation. *arXiv preprint arXiv:2506.18088*, 2025. 9
- [11] Zhangquan Chen, Xufang Luo, and Dongsheng Li. Visrl: Intention-driven visual perception via reinforced reasoning. *arXiv preprint arXiv:2503.07523*, 2025. 3
- [12] Zhangquan Chen, Manyuan Zhang, Xinlei Yu, Xufang Luo, Mingze Sun, Zihao Pan, Yan Feng, Peng Pei, Xunliang Cai, and Ruqi Huang. Think with 3d: Geometric imagination grounded spatial reasoning from limited views. *arXiv preprint arXiv:2510.18632*, 2025. 3
- [13] Zhangquan Chen, Ruihui Zhao, Chuwei Luo, Mingze Sun, Xinlei Yu, Yangyang Kang, and Ruqi Huang. Sifthinker: Spatially-aware image focus for visual reasoning. *arXiv preprint arXiv:2508.06259*, 2025. 3
- [14] Can Cui, Pengxiang Ding, Wenxuan Song, Shuanghao Bai, Xinyang Tong, Zirui Ge, Runze Suo, Wanqi Zhou, Yang Liu, Bofang Jia, et al. Openhelix: A short survey, empirical analysis, and open-source dual-system vla model for robotic manipulation. *arXiv preprint arXiv:2505.03912*, 2025. 1

-
- [15] Pengxiang Ding, Han Zhao, Wenjie Zhang, Wenxuan Song, Min Zhang, Siteng Huang, Ningxi Yang, and Donglin Wang. Quar-vla: Vision-language-action model for quadruped robots. In *European Conference on Computer Vision*, pages 352–367. Springer, 2024. 1
- [16] Pengxiang Ding, Jianfei Ma, Xinyang Tong, Binghong Zou, Xinxin Luo, Yiguo Fan, Ting Wang, Hongchao Lu, Panzhong Mo, Jinxin Liu, et al. Humanoid-vla: Towards universal humanoid control with visual integration. *arXiv preprint arXiv:2502.14795*, 2025. 1
- [17] Zhehao Dong, Xiaofeng Wang, Zheng Zhu, Yirui Wang, Yang Wang, Yukun Zhou, Boyuan Wang, Chaojun Ni, Runqi Ouyang, Wenkang Qin, et al. Emma: Generalizing real-world robot manipulation via generative visual transfer. *arXiv preprint arXiv:2509.22407*, 2025. 3
- [18] Yao Feng, Hengkai Tan, Xinyi Mao, Chendong Xiang, Guodong Liu, Shuhe Huang, Hang Su, and Jun Zhu. Vidar: Embodied video diffusion model for generalist manipulation. *arXiv preprint arXiv:2507.12898*, 2025. 6
- [19] Raghav Goyal, Samira Ebrahimi Kahou, Vincent Michalski, Joanna Materzynska, Susanne Westphal, Heuna Kim, Valentin Haenel, Ingo Fruend, Peter Yianilos, Moritz Mueller-Freitag, et al. The "something something" video database for learning and evaluating visual common sense. In *Proceedings of the IEEE international conference on computer vision*, pages 5842–5850, 2017. 6
- [20] Kristen Grauman, Andrew Westbury, Eugene Byrne, Zachary Chavis, Antonino Furnari, Rohit Girdhar, Jackson Hamburger, Hao Jiang, Miao Liu, Xingyu Liu, et al. Ego4d: Around the world in 3,000 hours of egocentric video. In *Proceedings of the IEEE/CVF conference on computer vision and pattern recognition*, pages 18995–19012, 2022. 6
- [21] Ryan Hoque, Peide Huang, David J Yoon, Mouli Sivapurapu, and Jian Zhang. Egodex: Learning dexterous manipulation from large-scale egocentric video. *arXiv preprint arXiv:2505.11709*, 2025. 6
- [22] Physical Intelligence, Kevin Black, Noah Brown, James Darpinian, Karan Dhabalia, Danny Driess, Adnan Esmail, Michael Equi, Chelsea Finn, Niccolo Fusai, et al. $\pi_{0.5}$: a vision-language-action model with open-world generalization. *arXiv preprint arXiv:2504.16054*, 2025. 1, 7, 8, 9, 10, 13
- [23] Tao Jiang, Tianyuan Yuan, Yicheng Liu, Chenhao Lu, Jianning Cui, Xiao Liu, Shuiqi Cheng, Jiyang Gao, Huazhe Xu, and Hang Zhao. Galaxea open-world dataset and g0 dual-system vla model. *arXiv preprint arXiv:2509.00576*, 2025. 1
- [24] Alexander Khazatsky, Karl Pertsch, Suraj Nair, Ashwin Balakrishna, Sudeep Dasari, Siddharth Karamcheti, Soroush Nasiriany, Mohan Kumar Srirama, Lawrence Yunliang Chen, Kirsty Ellis, et al. Droid: A large-scale in-the-wild robot manipulation dataset. *arXiv preprint arXiv:2403.12945*, 2024. 6
- [25] Moo Jin Kim, Yihuai Gao, Tsung-Yi Lin, Yen-Chen Lin, Yunhao Ge, Grace Lam, Percy Liang, Shuran Song, Ming-Yu Liu, Chelsea Finn, et al. Cosmos policy: Fine-tuning video models for visuomotor control and planning. *arXiv preprint arXiv:2601.16163*, 2026. 1, 2, 3, 7, 8, 9, 13
- [26] Seungwook Kim, Seunghyeon Lee, and Minsu Cho. Freeaction: Training-free techniques for enhanced fidelity of trajectory-to-video generation. *arXiv preprint arXiv:2509.24241*, 2025. 3
- [27] Haoyun Li, Ivan Zhang, Runqi Ouyang, Xiaofeng Wang, Zheng Zhu, Zhiqin Yang, Zhentao Zhang, Boyuan Wang, Chaojun Ni, Wenkang Qin, et al. Mimicdreamer: Aligning human and robot demonstrations for scalable vla training. *arXiv preprint arXiv:2509.22199*, 2025. 3
- [28] Hengtao Li, Pengxiang Ding, Runze Suo, Yihao Wang, Zirui Ge, Dongyuan Zang, Kexian Yu, Mingyang Sun, Hongyin Zhang, Donglin Wang, et al. Vla-rft: Vision-language-action reinforcement fine-tuning with verified rewards in world simulators. *arXiv preprint arXiv:2510.00406*, 2025. 1
-

- [29] Jiuming Liu, Ruiji Yu, Yian Wang, Yu Zheng, Tianchen Deng, Weicai Ye, and Hesheng Wang. Point mamba: A novel point cloud backbone based on state space model with octree-based ordering strategy. *arXiv preprint arXiv:2403.06467*, 2024. 3
- [30] Jiuming Liu, Jinru Han, Lihao Liu, Angelica I Aviles-Rivero, Chaokang Jiang, Zhe Liu, and Hesheng Wang. Mamba4d: Efficient 4d point cloud video understanding with disentangled spatial-temporal state space models. In *Proceedings of the Computer Vision and Pattern Recognition Conference*, pages 17626–17636, 2025. 3
- [31] Jiuming Liu, Mengmeng Liu, Siting Zhu, Yunpeng Zhang, Jiangtao Li, Michael Ying Yang, Francesco Nex, Hao Cheng, and Hesheng Wang. Arflow: Auto-regressive optical flow estimation for arbitrary-length videos via progressive next-frame forecasting. In *The Fourteenth International Conference on Learning Representations*, 2026. 1
- [32] Liu Liu, Xiaofeng Wang, Guosheng Zhao, Keyu Li, Wenkang Qin, Jiexiong Qiu, Zheng Zhu, Guan Huang, and Zhizhong Su. Robotransfer: Geometry-consistent video diffusion for robotic visual policy transfer. *arXiv preprint arXiv:2505.23171*, 2025. 3
- [33] Songming Liu, Lingxuan Wu, Bangguo Li, Hengkai Tan, Huayu Chen, Zhengyi Wang, Ke Xu, Hang Su, and Jun Zhu. Rdt-1b: a diffusion foundation model for bimanual manipulation. *arXiv preprint arXiv:2410.07864*, 2024. 6
- [34] Andrés Marafioti, Orr Zohar, Miquel Farré, Merve Noyan, Elie Bakouch, Pedro Cuenca, Cyril Zakka, Loubna Ben Allal, Anton Lozhkov, Nouamane Tazi, et al. Smolvlm: Redefining small and efficient multimodal models. *arXiv preprint arXiv:2504.05299*, 2025. 1
- [35] Chaojun Ni, Cheng Chen, Xiaofeng Wang, Zheng Zhu, Wenzhao Zheng, Boyuan Wang, Tianrun Chen, Guosheng Zhao, Haoyun Li, Zhehao Dong, et al. Swiftvla: Unlocking spatiotemporal dynamics for lightweight vla models at minimal overhead. *arXiv preprint arXiv:2512.00903*, 2025. 1, 2
- [36] Chaojun Ni, Jie Li, Haoyun Li, Hengyu Liu, Xiaofeng Wang, Zheng Zhu, Guosheng Zhao, Boyuan Wang, Chenxin Li, Guan Huang, et al. Wonderfree: Enhancing novel view quality and cross-view consistency for 3d scene exploration. *arXiv preprint arXiv:2506.20590*, 2025. 3
- [37] Chaojun Ni, Xiaofeng Wang, Zheng Zhu, Weijie Wang, Haoyun Li, Guosheng Zhao, Jie Li, Wenkang Qin, Guan Huang, and Wenjun Mei. Wonderturbo: Generating interactive 3d world in 0.72 seconds. *arXiv preprint arXiv:2504.02261*, 2025. 3
- [38] Chaojun Ni, Guosheng Zhao, Xiaofeng Wang, Zheng Zhu, Wenkang Qin, Xinze Chen, Guanghong Jia, Guan Huang, and Wenjun Mei. Recondreamer-rl: Enhancing reinforcement learning via diffusion-based scene reconstruction. *arXiv preprint arXiv:2508.08170*, 2025. 3
- [39] Chaojun Ni, Guosheng Zhao, Xiaofeng Wang, Zheng Zhu, Wenkang Qin, Guan Huang, Chen Liu, Yuyin Chen, Yida Wang, Xueyang Zhang, et al. Recondreamer: Crafting world models for driving scene reconstruction via online restoration. In *Proceedings of the Computer Vision and Pattern Recognition Conference*, pages 1559–1569, 2025. 3
- [40] Abby O’Neill, Abdul Rehman, Abhiram Maddukuri, Abhishek Gupta, Abhishek Padalkar, Abraham Lee, Acorn Pooley, Agrim Gupta, Ajay Mandlekar, Ajinkya Jain, et al. Open x-embodiment: Robotic learning datasets and rt-x models: Open x-embodiment collaboration 0. In *ICRA*, 2024. 6
- [41] Jonas Pai, Liam Achenbach, Victoriano Montesinos, Benedek Forrai, Oier Mees, and Elvis Nava. mimic-video: Video-action models for generalizable robot control beyond vlas. *arXiv preprint arXiv:2512.15692*, 2025. 2, 3

- [42] Dustin Podell, Zion English, Kyle Lacey, Andreas Blattmann, Tim Dockhorn, Jonas Müller, Joe Penna, and Robin Rombach. Sd-xl: Improving latent diffusion models for high-resolution image synthesis. *arXiv preprint arXiv:2307.01952*, 2023. 1
- [43] Yichao Shen, Fangyun Wei, Zhiying Du, Yaobo Liang, Yan Lu, Jiaolong Yang, Nanning Zheng, and Baining Guo. Videovla: Video generators can be generalizable robot manipulators. *arXiv preprint arXiv:2512.06963*, 2025. 1, 2, 3
- [44] Andreas Steiner, André Susano Pinto, Michael Tschannen, Daniel Keysers, Xiao Wang, Yonatan Bitton, Alexey Gritsenko, Matthias Minderer, Anthony Sherbondy, Shangbang Long, et al. Paligemma 2: A family of versatile vlms for transfer. *arXiv preprint arXiv:2412.03555*, 2024. 1
- [45] Aether Team, Haoyi Zhu, Yifan Wang, Jianjun Zhou, Wenzheng Chang, Yang Zhou, Zizun Li, Junyi Chen, Chunhua Shen, Jiangmiao Pang, et al. Aether: Geometric-aware unified world modeling. *arXiv preprint arXiv:2503.18945*, 2025. 3
- [46] GigaBrain Team, Angen Ye, Boyuan Wang, Chaojun Ni, Guan Huang, Guosheng Zhao, Haoyun Li, Jie Li, Jiagang Zhu, Lv Feng, et al. Gigabrain-0: A world model-powered vision-language-action model. *arXiv preprint arXiv:2510.19430*, 2025. 1, 7, 8, 9, 13
- [47] GigaBrain Team, Boyuan Wang, Chaojun Ni, Guan Huang, Guosheng Zhao, Hao Li, Jie Li, Jindi Lv, Jingyu Liu, Lv Feng, et al. Gigabrain-0.5 m*: a vla that learns from world model-based reinforcement learning. *arXiv preprint arXiv:2602.12099*, 2026. 1
- [48] GigaWorld Team, Angen Ye, Boyuan Wang, Chaojun Ni, Guan Huang, Guosheng Zhao, Haoyun Li, Jiagang Zhu, Kerui Li, Mengyuan Xu, et al. Gigaworld-0: World models as data engine to empower embodied ai. *arXiv preprint arXiv:2511.19861*, 2025. 3
- [49] Jingyi Tian, Le Wang, Sanping Zhou, Sen Wang, Jiayi Li, Haowen Sun, and Wei Tang. Pdfactor: Learning tri-perspective view policy diffusion field for multi-task robotic manipulation. In *Proceedings of the Computer Vision and Pattern Recognition Conference*, pages 15757–15767, 2025. 1
- [50] Team Wan, Ang Wang, Baole Ai, Bin Wen, Chaojie Mao, Chen-Wei Xie, Di Chen, Feiwu Yu, Haiming Zhao, Jianxiao Yang, Jianyuan Zeng, Jiayu Wang, Jingfeng Zhang, Jingren Zhou, Jinkai Wang, Jixuan Chen, Kai Zhu, Kang Zhao, Keyu Yan, Lianghua Huang, Mengyang Feng, Ningyi Zhang, Pandeng Li, Pingyu Wu, Ruihang Chu, Ruili Feng, Shiwei Zhang, Siyang Sun, Tao Fang, Tianxing Wang, Tianyi Gui, Tingyu Weng, Tong Shen, Wei Lin, Wei Wang, Wei Wang, Wenmeng Zhou, Wenten Wang, Wenting Shen, Wenyan Yu, Xianzhong Shi, Xiaoming Huang, Xin Xu, Yan Kou, Yangyu Lv, Yifei Li, Yijing Liu, Yiming Wang, Yingya Zhang, Yitong Huang, Yong Li, You Wu, Yu Liu, Yulin Pan, Yun Zheng, Yuntao Hong, Yupeng Shi, Yutong Feng, Zeyinzi Jiang, Zhen Han, Zhi-Fan Wu, and Ziyu Liu. Wan: Open and advanced large-scale video generative models. *arXiv preprint arXiv:2503.20314*, 2025. 2, 5, 6, 7
- [51] Boyuan Wang, Xinpan Meng, Xiaofeng Wang, Zheng Zhu, Angen Ye, Yang Wang, Zhiqin Yang, Chaojun Ni, Guan Huang, and Xingang Wang. Embodiedreamer: Advancing real2sim2real transfer for policy training via embodied world modeling. *arXiv preprint arXiv:2507.05198*, 2025. 3
- [52] Boyuan Wang, Runqi Ouyang, Xiaofeng Wang, Zheng Zhu, Guosheng Zhao, Chaojun Ni, Guan Huang, Lihong Liu, and Xingang Wang. Humandreamer-x: Photorealistic single-image human avatars reconstruction via gaussian restoration. *arXiv preprint arXiv:2504.03536*, 2025. 3
- [53] Boyuan Wang, Xiaofeng Wang, Chaojun Ni, Guosheng Zhao, Zhiqin Yang, Zheng Zhu, Muyang Zhang, Yukun Zhou, Xinze Chen, Guan Huang, Lihong Liu, and Xingang Wang. Humandreamer: Generating controllable human-motion videos via decoupled generation. *arXiv preprint arXiv:2503.24026*, 2025. 1, 3

- [54] Sen Wang, Jingyi Tian, Le Wang, Zhimin Liao, Jiayi Li, Huaiyi Dong, Kun Xia, Sanping Zhou, Wei Tang, and Hua Gang. Sampo: Scale-wise autoregression with motion prompt for generative world models. *arXiv preprint arXiv:2509.15536*, 2025. 3
- [55] Sen Wang, Le Wang, Sanping Zhou, Jingyi Tian, Jiayi Li, Haowen Sun, and Wei Tang. Flowram: Grounding flow matching policy with region-aware mamba framework for robotic manipulation. In *Proceedings of the Computer Vision and Pattern Recognition Conference*, pages 12176–12186, 2025. 1
- [56] Weijie Wang, Jiagang Zhu, Zeyu Zhang, Xiaofeng Wang, Zheng Zhu, Guosheng Zhao, Chaojun Ni, Haoxiao Wang, Guan Huang, Xinze Chen, et al. Drivegen3d: Boosting feed-forward driving scene generation with efficient video diffusion. *arXiv preprint arXiv:2510.15264*, 2025. 3
- [57] Yihao Wang, Pengxiang Ding, Lingxiao Li, Can Cui, Zirui Ge, Xinyang Tong, Wenxuan Song, Han Zhao, Wei Zhao, Pengxu Hou, Siteng Huang, Yifan Tang, Wenhui Wang, Ru Zhang, Jianyi Liu, and Donglin Wang. Vla-adapter: An effective paradigm for tiny-scale vision-language-action model. *arXiv preprint arXiv:2509.09372*, 2025. 1
- [58] Hao Wu, Hui Li, and Yiyun Su. Bridging the perception-cognition gap:re-engineering sam2 with hilbert-mamba for robust vlm-based medical diagnosis. In *2025 IEEE International Conference on Bioinformatics and Biomedicine (BIBM)*, pages 4275–4278, 2025. 1
- [59] Kun Wu, Chengkai Hou, Jiaming Liu, Zhengping Che, Xiaozhu Ju, Zhuqin Yang, Meng Li, YINUO Zhao, Zhiyuan Xu, Guang Yang, et al. Robomind: Benchmark on multi-embodiment intelligence normative data for robot manipulation. *arXiv preprint arXiv:2412.13877*, 2024. 6
- [60] Jiannan Xiang, Guangyi Liu, Yi Gu, Qiyue Gao, Yuting Ning, Yuheng Zha, Zeyu Feng, Tianhua Tao, Shibo Hao, Yemin Shi, et al. Pandora: Towards general world model with natural language actions and video states. *arXiv preprint arXiv:2406.09455*, 2024. 3
- [61] Angen Ye, Zeyu Zhang, Boyuan Wang, Xiaofeng Wang, Dapeng Zhang, and Zheng Zhu. Vla-r1: Enhancing reasoning in vision-language-action models. *arXiv preprint arXiv:2510.01623*, 2025. 1
- [62] Hua Ye, Siyuan Chen, Ziqi Zhong, Canran Xiao, Haoliang Zhang, Yuhan Wu, and Fei Shen. Seeing through the conflict: Transparent knowledge conflict handling in retrieval-augmented generation. *arXiv preprint arXiv:2601.06842*, 2026. 1
- [63] Wenyao Zhang, Hongsi Liu, Zekun Qi, Yunnan Wang, Xinqiang Yu, Jiazhao Zhang, Runpei Dong, Jiawei He, He Wang, Zhizheng Zhang, et al. Dreamvla: a vision-language-action model dreamed with comprehensive world knowledge. *arXiv preprint arXiv:2507.04447*, 2025. 1, 2
- [64] Guosheng Zhao, Chaojun Ni, Xiaofeng Wang, Zheng Zhu, Xueyang Zhang, Yida Wang, Guan Huang, Xinze Chen, Boyuan Wang, Youyi Zhang, et al. Drivedreamer4d: World models are effective data machines for 4d driving scene representation. In *Proceedings of the computer vision and pattern recognition conference*, pages 12015–12026, 2025. 3
- [65] Guosheng Zhao, Xiaofeng Wang, Chaojun Ni, Zheng Zhu, Wenkang Qin, Guan Huang, and Xingang Wang. Recondreamer++: Harmonizing generative and reconstructive models for driving scene representation. *arXiv preprint arXiv:2503.18438*, 2025. 3
- [66] Jinliang Zheng, Jianxiong Li, Zhihao Wang, Dongxiu Liu, Xirui Kang, Yuchun Feng, Yinan Zheng, Jiayin Zou, Yilun Chen, Jia Zeng, et al. X-vla: Soft-prompted transformer as scalable cross-embodiment vision-language-action model. *arXiv preprint arXiv:2510.10274*, 2025. 7, 13
- [67] Siyuan Zhou, Yilun Du, Jiaben Chen, Yandong Li, Dit-Yan Yeung, and Chuang Gan. Robodreamer: Learning compositional world models for robot imagination. *arXiv preprint arXiv:2404.12377*, 2024. 3